Simulation study on an improved frequency-doubled triangular-shaped pulse train generator with reduced harmonic distortion

Jing Li (李 晶)[1,2], TiGang Ning (宁提纲)[1,2], Li Pei (裴 丽)[1,2*], Jingjing Zheng (郑晶晶)[1,2], Yueqin Li (李月琴)[1,2], Jin Yuan (袁 瑾)[1,2], Yiqun Wang (王一群)[1,2], Chan Zhang (张 婵)[1,2], and Hongyao Chen (陈宏尧)[1,2]

[1]*Key Lab of All Optical Network & Advanced Telecommunication Network of EMC, Beijing Jiaotong University, Beijing 100044, China*

[2]*Institute of Lightwave Technology, Beijing Jiaotong University, Beijing 100044, China*

[*]*Corresponding author: lipei@bjtu.edu.cn*

Received July 8, 2014; accepted September 11, 2014; posted online November 17, 2014

An approach to reducing the harmonic distortion in frequency-doubled triangular-shaped pulse train generation is proposed. It requires a dual-parallel Mach–Zehnder modulator followed by a section of dispersive fiber, as the key component. The basic principle is to make the expression of optical intensity approximately equal to the Fourier expansion of idea triangular-shaped waveform. A detailed expression of the final optical intensity is given by theory and then verified by simulation. It is found that the impact of the undesired harmonic distortion is greatly reduced.

OCIS codes: 060.1155, 060.5625, 060.4080.
doi: 10.3788/COL201412.120602.

Photonic generation of triangular-shaped pulse, which is characterized by its linearly upping and falling edges in waveform, has already attracted many researcher's attention due to its applications in all-optical processing and manipulation (i.e., all-optical conversion, pulse compression, and signal copying)[1–4]. Various approaches have been proposed to generate triangular-shaped pulses. They can be classified into two major categories, one of which uses spectrum pulse shaping method[5–7], which requires pulse laser (or mode-locked laser) as light source. However, these prototypes suffer from expensive cost and poor repetition rate tunability. Besides, the generated pulse train has a small duty cycle (<1), which will need pulse stretch (duty cycle = 1) when used in time-division multiplexing to wavelength-division multiplexing conversion[3] or in pulse doubling[4]. The second category uses continuous wave (CW) laser as light source. For instance, Dai *et al.*[8] reported a versatile waveform generator based on comb generation. Using this technique, triangular-shaped pulses with tunable repetition rate can be generated. But the proposal requires large signal modulation to obtain comb-like spectrum. In Ref. [9], we reported a triangular-shaped pulse train generator using a dual-parallel Mach–Zehnder modulator (DP-MZM). Its key principle is to manipulate the frequency harmonics in the optical intensity roughly equal to the Fourier components of an idea triangular-shaped waveform, which to the best of our knowledge can be considered as the harmonic fitting employed in triangular-shaped pulse generation. However, since two radio frequency (RF) signals with different frequencies (f_{RF} and $3f_{\mathrm{RF}}$) are required in the RF modulation, the proposal is complex. The theory of harmonic fitting has already been used in recent research studies, for example, Pan *et al.*[10] proposed a triangular-shaped pulse train generator also using a DP-MZM. Unlike the prototype in Ref. [9], it requires only one RF signal (f_{RF}) as the driving signal, which will simplify the setup., Then Liu *et al.*[11] reported an optical triangular waveform generator using a polarization modulator (PolM) in a Sagnac loop and Li *et al.*[12] proposed a photonic approach to generate triangular-shaped waveform signal based on a DP-MZM and optical filtering technique. These approaches in Refs. [8–12] are simple and characterized by continuous tunability of repetition rate. However, the disadvantage is that the repetition rate of generated pulse train is pretty low, equal to the driving frequency. Since an electro-optical modulator (MZM or PolM) is the basic component in these schemes[8–12], the repetition rate tunable range is highly limited by the bandwidth of the modulator. Then in Ref. [13], we used a dual-drive Mach–Zehnder modulator (DD-MZM) to generate lightwaves with frequency-doubled optical carrier suppressed (OCS) modulation, then a section of dispersive fiber was connected to remove the undesired 4th harmonic in optical intensity. However, due to the extinction ratio of the modulator, undesired harmonic distortion is very strong, which will lead to power oscillation and waveform distortion of the generated pulse train. Thus, the fiber dispersion is required to be properly adjusted (i.e., $\beta_2 L = -5\pi/8\Omega^2$). In that case, the impact can be reduced to some extent. Later, Li *et al.*[14] reported an approach to generating full duty-cycle triangular waveform based on a microwave photonic filter (MPF) with negative coefficient in their latest research.

The pulse repetition rate is also two times that of driving frequency. But the approach based on a MPF can only generate electrical pulse train, not optical one. Additional electrical-to-optical conversion is required for all-optical processing application.

In this work, another approach to reduce that impact is proposed and analyzed. It requires a DP-MZM (also known as a $LiNbO_3$ DQPSK modulator) followed by a section of single-mode fiber (SMF), as the key component. Different from the DD-MZM, one typical DP-MZM consists of two child MZMs (MZM-a and MZM-b) embedded on the parent MZM (MZM-c). To realize the OCS modulation, MZM-a, MZM-b, and MZM-c should be all biased at the minimum transmission point (MITP). After modulation, there will be less undesired optical sidebands left in optical spectrum. Less undesired optical sideband also means less harmonic distortion in optical intensity. In our case, the improvement is conductive to a stable pulse train generation, for instance, the power oscillation of the pulse train will be much smaller and the shape will be much closer to the idea triangular-shaped waveform. To investigate its mechanism, a detailed expression of optical intensity is given. The performance of generator is analyzed by theory and then verified by simulation. It is shown that the harmonic distortion can be greatly reduced (from 16% to less than 16%).

Figure 1 shows the schematic diagram of the proposed frequency-doubled triangular-shaped pulse train generator. The key component is a DP-MZM followed by a section of SMF. The modulator consists of two child MZMs, that is, MZM-a in upper branch and MZM-b in lower branch, and a parent MZM (MZM-c). Because of the x-cut design, they are configured for the push–pull operation, and each has independent DC bias.

Suppose that the driving signals from the local oscillator (LO) is $V_{\mathrm{LO}}(t) = V_{\mathrm{LO}}\sin\Omega t$, where V_{LO} and $\Omega = 2\pi f_{\mathrm{RF}}$ are the magnitude and angular frequency of LO. It is assumed that the extinction ratios of all three MZMs are identical. To realize OCS modulation, all three MZMs should be biased at MITP ($V_{\text{bias-a}} = V_{\text{bias-b}} = V_{\text{bias-c}} = V_\pi$). In that case, optical field at the output of DP-MZM can be concluded as

$$\begin{aligned} E_1(t) &= \frac{E_0(t)}{2\sqrt{t_{ff}}}\left\{\gamma^2\exp\left[j\frac{V_{\mathrm{LO}}}{2V_\pi}\sin\Omega t\right]-\gamma(1-\gamma)\exp\left[-j\frac{V_{\mathrm{LO}}}{2V_\pi}\sin\Omega t\right]\right. \\ &\quad -\gamma(1-\gamma)\exp\left[-j\frac{V_{\mathrm{LO}}}{2V_\pi}\sin\Omega t\right] \\ &\quad \left.+(1-\gamma)^2\exp\left[-j\frac{V_{\mathrm{LO}}}{2V_\pi}\sin\Omega t\right]\right\} \\ &= \frac{E_{\mathrm{in}}(t)}{2\sqrt{t_{ff}}}\sum_{n=-\infty}^{\infty}a_n\exp(jn\Omega t), \end{aligned} \tag{1}$$

where optical sideband magnitude is

$$a_n = \left[\gamma^2-2(-1)^n\gamma(1-\gamma)+(1-\gamma)^2\right]J_n\left(\frac{V_{\mathrm{LO}}}{2V_\pi}\right), \tag{2}$$

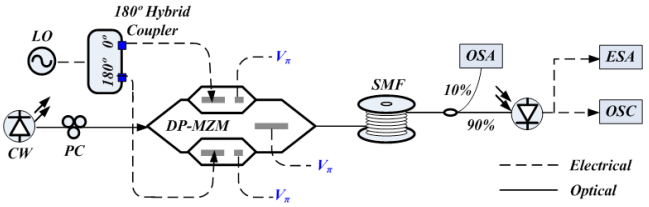

Fig. 1. Schematic diagram of the proposed frequency-doubled triangular-shaped pulse train generator with reduced harmonic distortion using a DP-MZM. PC, polarization controller; OSA, optical spectrum analyzer; ESA, electrical spectrum analyzer; OSC, oscilloscope.

and $E_0(t) = E_0\exp(j\omega_0 t)$ represents the input optical field, where E_0 and ω_0 denote its amplitude and angular frequency, and t_{ff} is the modulator's insertion loss. $\Gamma = (1-1/\sqrt{\varepsilon_{\mathrm{r}}})/2$ represents the power splinting (combining) ratio for the input and output Y-branch waveguides, where ε_{r} is the extinction ratio. Besides, the parameter $m=\pi V_{\mathrm{LO}}/2V_\pi$ is defined as the modulation index, where V_π is the half-wave switching voltage of DP-MZM. Note that even-order harmonic sidebands (in Eq. (2)) are almost suppressed, that is, n = even number. Then the lightwave is coupled to a section of SMF. Its transmission function can be found in Ref. [15] (neglecting the constant phase and higher order terms). Then the optical field becomes

$$E_2(t) \propto \sum_{n=-\infty}^{\infty}a_n\exp\left(jn\Omega t + j\frac{1}{2}n^2\beta_2 L\Omega^2\right), \tag{3}$$

where $\beta_2 = -\lambda_0^2 D/(2\pi c)$, λ_0 is the optical wavelength, c is the speed of light in vacuum, L is the fiber length, and D is the chromatic dispersion parameter. As has been demonstrated in Ref. [9], to obtain triangular-shaped waveform, the modulation index should be adjusted to $m = 2.305$. In that case, the optical sidebands higher than 3rd order ($|n|>3$) are negligible. Thus, by only considering optical sidebands with order of up to 3rd ($|n|\le 3$) in $E_2(t)$, optical intensity as a function of Ω can be concluded as

$$\begin{aligned} I(t) \propto & \underbrace{\left[\frac{1}{2}a_0^2+\sum_{n=1}^{3}a_n^2\right]-\left[a_1^2\cos(2\Omega t)+a_3^2\cos(6\Omega t)\right]}_{\text{Desired Harmonics}} \\ & \underbrace{-\left[I_\Omega\sin(\Omega t)+I_{3\Omega}\sin(3\Omega t)\right.}_{} \\ & \underbrace{\left.+I_{4\Omega}\sin(4\Omega t)+I_{5\Omega}\sin(5\Omega t)\right]}_{\text{Undesired Harmonics}}. \end{aligned} \tag{4}$$

In the expression of optical intensity $I(t)$, the magnitude of the undesired harmonics (I_Ω, $I_{3\Omega}$, $I_{4\Omega}$, and $I_{5\Omega}$) can be considered as the distortion:

$$\begin{aligned} I_\Omega &= 2a_0a_1\sin\left(\frac{1}{2}\beta_2 L\Omega^2\right)+2a_1a_2\sin\left(\frac{3}{2}\beta_2 L\Omega^2\right) \\ &\quad +2a_2a_3\sin\left(\frac{5}{2}\beta_2 L\Omega^2\right), \end{aligned} \tag{5}$$

$$I_{3\Omega} = 2a_0a_3\sin\left(\frac{9}{2}\beta_2 L\Omega^2\right)-2a_1a_2\sin\left(\frac{3}{2}\beta_2 L\Omega^2\right), \tag{6}$$

$$I_{4\Omega} = 2a_1a_3\cos\left(4\beta_2 L\Omega^2\right) - a_2^2 \ , \tag{7}$$

$$I_{5\Omega} = 2a_2a_3\sin\left(\frac{5}{2}\beta_2 L\Omega^2\right) . \tag{8}$$

As stated in Eq. (2), the magnitude of even-order sideband (n = even number) is negligible. Thus, the primary distortion is induced by the 4th order harmonic. To minimize that impact, the fiber dispersion should be adjusted to

$$\left|\beta_2 L\right| = \frac{(2k+1)\pi}{8\Omega^2} \ , \qquad k = 0,\ 1,\ 2,\ 3,... \tag{9}$$

By substituting Eq. (9) into Eqs. (5)–(8), we will focus on the impact of undesired harmonic. To do this, we have to calculate the upper limit (i.e., maximum value) of $I_1(t)$ and $I_2(t)$, where $I_1(t)$ represents the desired harmonics and $I_2(t)$ denotes the undesired harmonics ($I_{4\Omega}$ is considered as negligibly small), as

$$I_{1,\max} = \frac{1}{2}a_0^2 + 2a_1^2 + a_2^2 + 2a_3^2 \tag{10}$$

$$I_{2,\max} = \left|I_{\Omega} - I_{3\Omega} + I_{5\Omega}\right| . \tag{11}$$

Figure 2 shows the ratio of $I_{2,\max}/I_{1,\max}$, which represents the impact of harmonic distortion versus the coefficient k in Eq. (9) at ε_r of 20, 25, 30, and 35 dB. As a comparison, Fig. 2(a) shows the results using a DD-MZM has been demonstrated in Ref. [13]. When ε_r is higher than 20 dB, the harmonic distortion can be controlled within 16%. Figure 2(b) shows the results using a DP-MZM. Note that the harmonic distortion has been greatly reduced (less than 16‰). By using our work, it is even unnecessary to adjust the dispersion coefficient k, since the existing distortion is too small that no extra procedure is required. This feature may be useful in case the driving frequency is required to be low (i.e., f = 5 GHz). Using the approach in Ref. [13], the optimum dispersion ($|\beta_2 L|$ = 1989.4 ps^2 at f = 5 GHz) is at least five times more than this work ($|\beta_2 L|$ = 397.88 ps^2 at f = 5 GHz).

To investigate the impact of harmonic distortion, Fig. 3 shows the temporal waveform of $I(t)$ (e.g., taking ε_r = 25 dB and k = 0 in Eq. (9)). The bold line denotes the result in Ref. [9]. Note that a relative high-power oscillation exists in the temporal waveform (bold line). Besides, it can be simply measured that the primary distortion comes from the 1st order harmonic, sinΩt. In our work (dotted line), the power level of pulse train is stable. Thus, the stability of the generated pulse train has been improved by using our work.

According to the pre-condition in Eq. (9) (i.e., k = 0), Fig. 4 illustrates the required dispersion $\beta_2 L$ versus driving frequency $f_{\rm RF}$. Using this relationship, the repetition rate's tunability can be realized by tuning $\beta_2 L$ and $f_{\rm RF}$, simultaneously. For instance, when $f_{\rm RF}$ is tuned to 10, 20, and 30 GHz, the required $\beta_2 L$ is supposed to be adjusted to –99.5, –24.9, and –11.1 ps^2, respectively.

Without considering the distortion, the optical intensity in Eq. (4) can be rewritten as

$$I(t) \propto \left[\frac{1}{2}a_0^2 + \sum_{n=1}^{3} a_n^2\right] - a_1^2\left[\cos(2\Omega t) + \frac{a_3^2}{a_1^2}\cos(6\Omega t)\right] . \tag{12}$$

When modulation index m is adjusted to 2.305, we can get $a_1^2 = 9a_3^2$. Considering $\omega = 2\Omega$, we can express an idea triangular-shaped pulse train, $T(t)$, by using $I(t)$ in Eq. (12) as

$$T(t) \propto \sum_{n=1}^{\infty}\frac{1}{(2n-1)^2}\cos\left[(2n-1)\cdot\omega t\right] = \cos(\omega t) + \frac{1}{9}\cos(3\omega t) + \frac{1}{25}\cos(5\omega t) + \cdots \tag{13}$$

Note that only two harmonics (ω and 3ω) are employed to fit the idea triangular-shaped waveform in our case (in Eq. (12)), which corresponds to n = 2 in Eq. (13). As a comparison, Fig. 5 shows the calculated gradient of $T(t)$ at different n = 2, 3, 10. It is shown that the gradients are supposed to be constant across the up- and falling edge of the pulse train once the coefficient n is equal to 10. However, such a difference is small since the high-order harmonics (5ω, 7ω, and so on) have a small contribution on the final waveform. Therefore, the output optical intensity is characterized by triangular-shaped waveform. The repetition rate is two times that of driving frequency $f_{\rm RF}$.

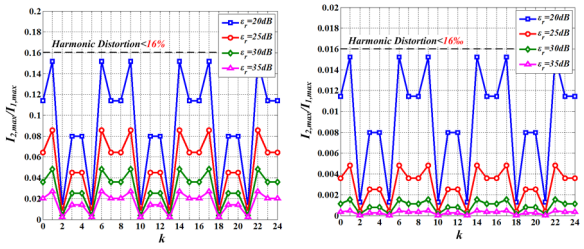

Fig. 2. Ratio of $I_{2,\max}/I_{1,\max}$ versus the coefficient k at ε_r of 20, 25, 30, and 35 dB using the approach in (a) Ref. [9] and (b) this work.

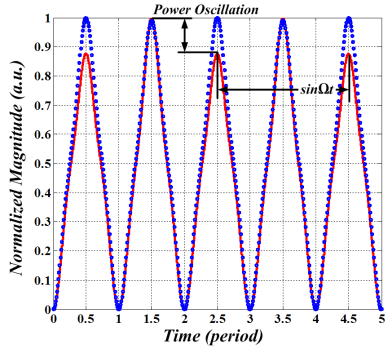

Fig. 3. Temporal waveform of $I(t)$ using the approach in Ref. [9] (bold line) and this work (dotted line). ε_r = 25 dB and k = 0 in Eq. (9).

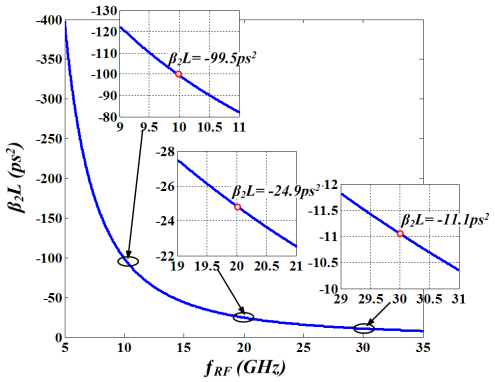

Fig. 4. Required dispersion $\beta_2 L$ versus driving frequency f_{RF} according to Eq. (9) and $k = 0$.

We compare and verify two approaches, one in Ref. [13] and one in our work, by simulation. The software we use is Opti-System 10.0. All parameters' setting are listed in Table 1.

In Case A, a lightwave from a CW laser source at center wavelength of 1550 nm, power of 10 dBm, and linewidth of 0.8 MHz is coupled to a DD-MZM. The modulator has an insertion loss of t_{ff} = 4.5 dB, a half-wave voltage of RF $V_{\pi\text{-RF}}$ = 4 V, a half-wave voltage of DC $V_{\pi\text{-DC}}$ = 10 V, and an extinction ratio ε_{r} = 25 dB. To realize the OCS modulation, the bias state of DD-MZM is supposed to be MITP, which means V_{bias} = 10 V. Then a RF signal operating at a frequency of f_{RF} = 10 GHz is firstly applied to a 180° hybrid coupler and then drive the modulator. The applied LO voltage is V_{LO} = 4.15 V, corresponding to the modulation index $m = \pi V_{\mathrm{LO}}/\sqrt{2}\, V_{\pi\text{-RF}}$ = 2.305. Then the lightwave is coupled to a section of SMF ($\beta_2 L$ = −99.5 ps²). Optical spectrum and temporal waveform are captured by an optical spectrum analyzer (resolution bandwidth 0.005 nm) and an ultra-high-speed oscilloscope (sample rate 1.28 THz). Besides, we use a broadband photodiode to detect the pulse train. An electrical spectrum analyzer is used to measure the electrical spectrum. All the results are shown in Figs. 6(a), (c), and (e). As demonstrated

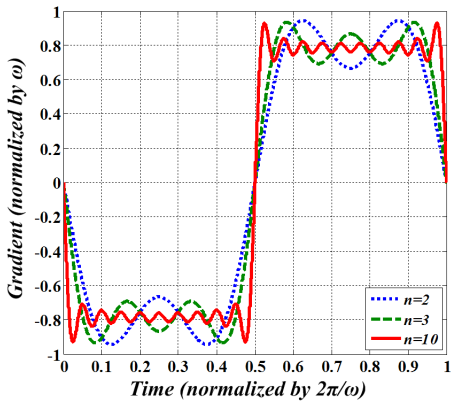

Fig. 5. Calculated gradient (normalized by ω) of $T(t)$ at different n = 2, 3, 10.

Table 1. Parameters' Setting

Symbol	Case A	Case B
λ_0	1550 nm	1550 nm
P_{in}	10 dBm	10 dBm
Δ	0.8 MHz	0.8 MHz
ε_{r}	25 dB	25 dB
t_{ff}	4.5 dB	4.5 dB
$V_{\pi\text{-DC}}$	10 V	10 V
V_{bias}	10 V	–
$V_{\mathrm{bias\text{-}a}}$	–	10 V
$V_{\mathrm{bias\text{-}b}}$	–	10 V
$V_{\mathrm{bias\text{-}c}}$	–	10 V
$V_{\pi\text{-RF}}$	4 V	4 V
V_{LO}	4.15 V	5.87 V
f_{RF}	10 GHz	10 GHz
β_2	−20 ps²/km	−20 ps²/km
L	4.975 km	4.975 km
α	0.2 dB/km	0.2 dB/km

Case A represents the approach in Ref. [13] and Case B in this work.

in Refs. [8–13], we only need to focus on the power difference between ±1st and ±3rd order sidebands in Fig. 6(a), and make sure it is roughly 9.5 dB. It has to be mentioned that the harmonic distortion is induced by the undesired even-order (±2 and ±4) optical sidebands in Fig. 6(a). In Fig. 6(c), the distortion is characterized by power oscillation of pulse train, which agrees well with the calculated results in Fig. 3. The harmonic feature of $I(t)$ can be observed in Fig. 6(e). Power difference between the 2nd and the 6th order harmonics is around 19 dB, which also agrees well with the experimental results in Ref. [10]. The undesired harmonics include 1st, 3rd, and 5th orders, which will be removed by using our work.

As a comparison, in Case B, we replace the DD-MZM with a DP-MZM. As shown in Fig. 1, a lightwave from a CW laser source at a central wavelength of 1550 nm, power of 10 dBm, and a linewidth of 0.8 MHz is coupled to a DP-MZM. The DP-MZM has an insertion loss of t_{ff} = 4.5 dB, a half-wave voltage of V_{π} = 4 V, and an extinction ratio ε_{r} = 25 dB. As stated above, MZM-a, MZM-b, and MZM-c are all biased at MITP, $V_{\mathrm{bias\text{-}a}} = V_{\mathrm{bias\text{-}b}} = V_{\mathrm{bias\text{-}c}}$ = 10 V. A RF signal operating at a frequency of

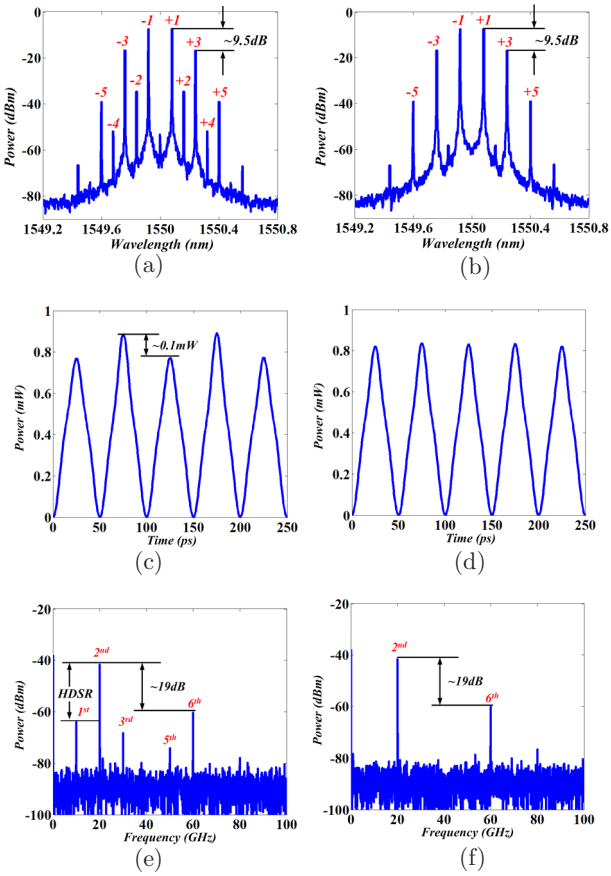

Fig. 6. Simulation results using the approach in Ref. [13]: (a) optical spectrum, (c) temporal waveform, and (e) electrical spectrum. Simulated results using the approach in this work: (b) optical spectrum, (d) temporal waveform, and (f) electrical spectrum.

f_{RF} = 10 GHz is firstly applied to a 180° hybrid coupler and then drive MZM-a and MZM-b. The applied LO voltage V_{LO} = 5.87 V, corresponding to modulation index $m = \pi V_{LO}/2V_{\pi\text{-RF}} = 2.305$. Then the lightwave is coupled to a section of SMF ($\beta_2 L$ = −99.5 ps²). Simulation results are shown in Figs. 6(b), (d), and (f). Note that even-order optical sidebands are fully suppressed (in Fig. 6(a)). Thus, there is less harmonic distortion in temporal waveform (in Fig. 6(d)). The problem of pulse train's power oscillation can be solved. Figure 6(f) shows the electrical spectra of signals after photodetection. As shown Fig. 6(f), only the 2nd and the 6th order harmonics exist. The power difference between is still 19 dB. Different from the results in Fig. 6(e), the undesired harmonics (1st, 3rd, and 5th) have been greatly reduced.

To verify the repetition rate's tunability, the following four cases are considered (according to Fig. 4): (a) f_{RF} = 15 GHz and $\beta_2 L$ = −44.2 ps², (b) f_{RF} = 20 GHz and $\beta_2 L$ = −24.9 ps², (c) f_{RF} = 25 GHz and $\beta_2 L$ = −15.9 ps², and (d) f_{RF} = 30 GHz and $\beta_2 L$ = −11.1 ps². Figures 7(a)–(d) show the simulated temporal waveform of $I(t)$ at different repetition rates corresponding to the above four cases. With this good performance can be

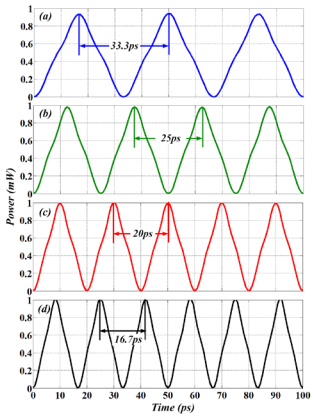

Fig. 7. Simulated temporal waveform of optical intensity with repetition rates of: (a) 30, (b) 40, (c) 50, and (d) 60 Gb/s.

observed. The repetition rate can be extended to 80 Gb/(s) since $LiNbO_3$ modulator with bandwidth 40 GHz is commercially available.

Since our prototype uses a DP-MZM as the key component, it is quite necessary to discuss the issue of bias-drifting problem. As shown in Fig. 1, one typical DP-MZM has three independent bias voltages. In our case, all three sub-MZMs are biased at the minimum transmission point, which should be all set as V_π. Here the bias voltage drift ratio is defined as $(\Delta V/V_\pi)\times 100\%$, where ΔV is the voltage drift and V_π is the half-wave voltage. To evaluate its impact, a harmonic distortion suppression ratio (HDSR) is defined as the power ratio of the 2nd order harmonic and the primary undesired harmonic. For example, in Fig. 6(e) the HDSR is the power ratio of the 2nd order harmonic and the 1st order harmonic, which is obtained as HDSR ≈ 23 dB.

Since the waveform of $I(t)$ is highly dependent on HDSR and the relationship between the 2nd and the 6th order harmonics, Fig. 8(a) illustrates the simulated $P_{2\Omega}/P_{6\Omega}$ and HDSR versus MZM-a bias voltage drifts $(\Delta V_1/V_\pi)\times 100\%$. Note that $P_{2\Omega}/P_{6\Omega}$ almost remains constant and the HDSR declines from 44 to 25 dB when bias drift is from -10% to 10%. Figure 8(b) shows the simulated $P_{2\Omega}/P_{6\Omega}$ and HDSR versus MZM-b bias voltage drifts $(\Delta V_2/V_\pi)\times 100\%$. Similar to that in Fig. 8(a), the power ratio between the 2nd and the 6th order harmonic $(P_{2\Omega}/P_{6\Omega})$ remains constant. The HDSR declines from 44 to 25 dB when bias drift is from -10% to 10%. Figure 8(c) shows the HDSR of the simulated $P_{2\Omega}/P_{6\Omega}$ and HDSR versus MZM-c bias voltage drifts $(\Delta V_3/V_\pi)\times 100\%$. Differing from the voltage drift of MZM-a and MZM-b, the HDSR decreases from around 44 to 37.5 dB when bias drift is from −10% to 10%. In our case, bias voltage deviation is roughly 2 V corresponding to drift of ±10%. In practice, the impact of DC-bias drifting can be reduced to a negligible amount by using a modulator with a large DC V_π.

In conclusion, a photonic approach to reduce the harmonic distortion in frequency-doubled triangular-shaped pulse train generation is proposed and verified

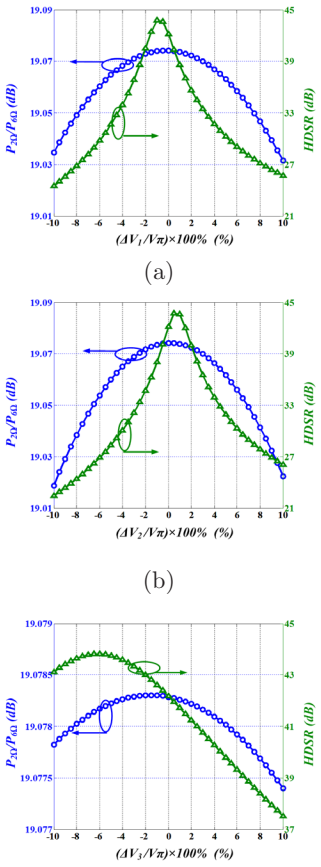

Fig. 8. Simulated $P_{2\Omega}/P_{6\Omega}$ and HDSR versus MZM bias voltage: (a) MZM-a bias drift, (b) MZM-b bias drift, and (c) MZM-c bias drift.

by simulation. The target pulse train generation requires one DP-MZM followed by a section of SMF. By setting modulation index $m = 2.305$ and fiber dispersion $\beta_2 L = -1\pi/8\Omega^2$ in Eq. (9), triangular-shaped pulse train with repetition rate two times of driving frequency can be generated. Different from previous work, this approach utilizes a DP-MZM instead of a DD-MZM. According to the analysis, with proper components configuration and bias control, undesired harmonic distortion can be greatly reduced (from 16% to less than 16‰). Compared with previous approach using a DD-MZM, it is even unnecessary to adjust the dispersion coefficient k, since the existing distortion is too small that no extra procedure is required. It is found that the power oscillation induced by harmonic distortion is removed by using our work and when the bias drift is controlled within ±10%, the output pulse train can be guaranteed with triangular-shaped waveform. The results also agree well with the theory and other experimental results, which make this approach more reliable in practical use. A disadvantage of our proposal is the repetition rate's tunability. Usually, to obtain a triangular-shaped pulse train with a certain repetition rate, the dispersion has to be properly chosen according to Eq. (9). In practice, tuning the dispersion seems to be quite difficult. Therefore, we have to adjust the CW laser's central wavelength, so as to precisely control the dispersion. As a matter of fact, such a procedure is quite necessary when driving frequency is pretty high.

This work was supported by the National Natural Science Foundation of China (No. 61405007), the Fundamental Research Funds for the Central Universities (No. 2014JBM013), and the Research Foundation for Talented Scholars of Beijing Jiaotong University(No. 2013RC021).

References

1. A. I. Latkin, S. Boscolo, R. S. Bhamber, and S. K. Turitsyn, in *Proceedings of 34th European Conference on Optical Communication* (2008).
2. F. Parmigiani, M. Ibsen, T. T. Ng, L. A. Provost, P. Petropoulos, and D. J. Richardson, in *Proceedings of 2008 Optical Fiber Communication Conference* (2008).
3. R. S. Bhamber, A. I. Latkin, S. Boscolo, and S. K. Turitsyn, in *Proceedings of 34th European Conference on Optical Communication* (2008).
4. A. I. Latkin, S. Boscolo, R. S. Bhamber, and S. K. Turitsyn, J. Opt. Soc. Am. B **26,** 1492 (2009).
5. S. Boscolo, A. I. Latkin, and S. K. Turitsyn, IEEE J. Quant. Electron. **44,** 1196 (2008).
6. J. Ye, L. Yan, W. Pan, B. Luo, X. Zou, A. Yi, and S. Yao, Opt. Lett. **36,** 1458 (2011).
7. Y. Park, M. H. Asghari, T.-J. Ahn, and J. Azaña, Opt. Express **15,** 9584 (2007).
8. B. Dai, Z. Gao, X. Wang, N. Kataoka, and N. Wada, Electron. Lett. **47,** 336 (2011).
9. J. Li, T. Ning, L. Pei, W. Peng, N. Jia, Q. Zhou, and X. Wen, Opt. Lett. **36,** 3828 (2011).
10. F. Zhang, X. Ge, and S. Pan, Opt. Lett. **38,** 4491 (2013).
11. W. Liu, L. Gao, and J. Yao, in *Proceedings of International Topical Meeting on Microwave Photonics* 68 (2013).
12. W. Li, W. T. Wang, and N. H. Zhu, IEEE Photon. J. **6,** 1 (2014).
13. J. Li, X. Zhang, B. Hraimel, T. Ning, L. Pei, and K. Wu, J. Lightw. Technol. **30,** 1617 (2012).
14. W. Li, W. T. Wang, W. H. Sun, W. Y. Wang, and N. H. Zhu, Opt. Express **22,** 14993 (2014).
15. G. Meslener, IEEE J. Quant. Electron. **20,** 1208 (1984).